

# Vancomycin Sorption on Pristine and Oxidized Exfoliated Graphite Nanoplatelets

ELENA RADU<sup>1</sup>, RUSANDICA STOICA<sup>1</sup>, SANDA MARIA DONCEA<sup>1</sup>, GABRIEL VASILIEVICI<sup>1</sup>, ELENA EMILIA OPRESCU<sup>2</sup>, ION BOLOCAN<sup>2</sup>, AHMED JASSIM MUKLIVE AL-OGAIDI<sup>3,4</sup>, ION ION<sup>3</sup>, ALINA CATRINEL ION<sup>3\*</sup>

<sup>1</sup> National Research & Development Institute for Chemistry and Petrochemistry ICECHIM, Department of Bioresources, 202 Splaiul Independentei Str., 060021, Bucharest, Romania

<sup>2</sup> Petroleum-Gas University of Ploiesti, Chemistry Department, 39 Bucharest Av., 100680, Ploiesti, Romania

<sup>3</sup> University Politehnica of Bucharest, Department of Analytical Chemistry and Environmental Engineering, 1-7 Polizu Str., 011061, Bucharest, Romania

<sup>4</sup> University of Technology, Department of Applied Sciences, Al-Senaa Str., Baghdad, Iraq

*Vancomycin (VCM) is an important antibiotic, very efficient in the treatment of severe infections caused by methicillin-resistant staphylococcus. High concentrations could cause severe side effects, being very important to determine the adequate VCM concentration levels in human biological fluids. This paper presents the experimental results regarding the adsorption capacity of new type of sorbents based on carbon nanomaterials such exfoliated graphite nanoplatelets (xGnP) and oxidized exfoliated graphite nanoplatelets (ox-xGnP) in aqueous solutions. The process can be used as a promising alternative for preconcentration before determination of the amount of VCM in biological fluids. The effect of different conditions such as: contact time, initial VCM concentration, temperature were tested, kinetic and sorption isotherms being established. A spectrophotometric method with UV detection at 220 nm was used to monitor the VCM concentration. The characterization of the nanomaterials, by FTIR and thermogravimetry, is shown in relevant comparative diagrams, before and after the adsorption experiments, in order to prove the good capacity of xGnP/ox-xGnP nanosheets to retain the molecules of VCM.*

**Keywords:** Vancomycin, methicillin-resistant staphylococcus, biological fluids, adsorption capacity, exfoliated graphite nanoplatelets

Vancomycin (VCM) is a glycopeptide antibiotic, isolated for the first time in 1956, by pharmaceutical company "Lilly Laboratory" from USA, in research studies on *Streptomyces orientalis* cultures, and introduced in medical clinics in 1958 [1]. VCM is an antibiotic used in the treatment of *Staphylococcus aureus* and *Staphylococcus epidermitis*, or other gram-positive infections for which drugs, such as penicillin G, are inefficient [1]. VCM is used for the treatment of infections caused by sensitive gram-positive organisms, for patients that are allergic to penicillins and cephalosporins [2]. Abuse of antibiotics leads to apparition of the new strains of bacteria which are naturally resistant to antibiotics, in the medical field being unanimously accepted that VCM is a very important alternative for methicillin-resistant staphylococcus and also for serious infections caused by *Clostridium difficile*.

The tricyclic structure of vancomycin was discovered in the late 70<sup>s</sup>, based on a high molecular weight glycopeptide of 1449.25 g mol<sup>-1</sup>. VCM is available as stable and highly soluble in the hydrochloride form, with chemical formula C<sub>66</sub>H<sub>73</sub>Cl<sub>2</sub>N<sub>9</sub>O<sub>24</sub>·HCl and molecular weight 1485.71 g mol<sup>-1</sup>. Structural formula is shown in figure 1.

From pharmaceutical point of view, the active form of vancomycin hydrochloride is as free base, without hydrochloric acid molecule. Vancomycin is commercially synthesised as hydrochloride, but active ingredient doses are expressed in terms of the base. 1.03 g of vancomycin hydrochloride is equivalent to 1 g of vancomycin (VCM) free base [1]. The real VCM concentration is calculated taking in account the conversion mass factor (1.03), purity and humidity of the active substance.

Vancomycin is intravenously injected, because it is not orally or intramuscular absorbed, and can cause pains or

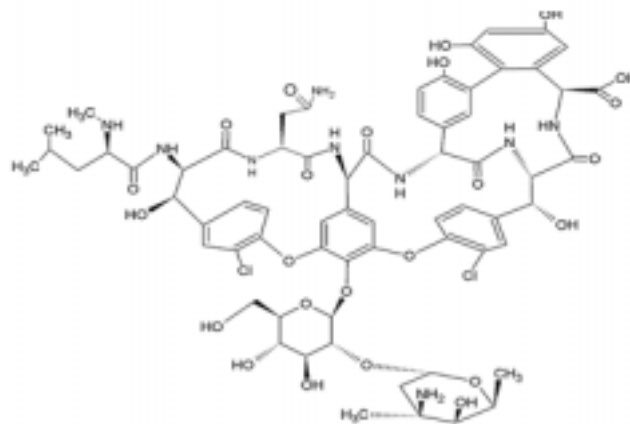


Fig.1. The structure of Vancomycin

muscle tissue necrosis. Monitoring of VCM concentration in biological fluids, blood and urine is very important, because high concentrations could cause severe side effects [4]. The major problem in vancomycin treatment is possible damage of the auditive nerve, when its concentration in blood exceeds 80 mg L<sup>-1</sup> and for renal toxicity, when the serum vancomycin concentration exceeds 10 mg L<sup>-1</sup> [5, 6]. The appropriate dose of VCM is in the range 5 - 10 mg L<sup>-1</sup>. To reduce the toxicity, it is recommended a seric concentration below 40 mg L<sup>-1</sup> [7]. Therefore, it is necessary to determine vancomycin concentration in biological fluids, in order to adjust its concentration in blood, for minimizing side effects.

The goal of this study is to determine the adsorption capacity of a new type of sorbents based on carbon nanomaterials with affinity for vancomycin. Experimental results have shown that exfoliated graphite nanoplatelets

\* email: ac\_ion@yahoo.com; Tel.: +40723295334

No.	Method	Detection system	LOD	Linearity range	Ref.
1.	Spectrophotometric	UV, $\lambda = 725$ nm	0.0156 $\mu\text{g mL}^{-1}$	2-18 $\mu\text{g mL}^{-1}$	[16]
2.	Spectrophotometric	UV, $\lambda = 240$ nm	2.7 $\mu\text{g mL}^{-1}$	4-32 $\mu\text{g mL}^{-1}$	[10]
3.	Spectrophotometric	UV, $\lambda = 620$ nm	1.13 $\times 10^{-2}$ $\mu\text{g mL}^{-1}$	1.15-3.11 $\mu\text{g mL}^{-1}$	[17]
4.	Spectrophotometric	UV, $\lambda = 520$ nm	5 $\times 10^{-2}$ $\mu\text{g mL}^{-1}$	2-24 $\mu\text{g mL}^{-1}$	[17]
5.	Spectrophotometric	UV, $\lambda = 540$ nm	5 $\times 10^{-2}$ $\mu\text{g mL}^{-1}$	2-24 $\mu\text{g mL}^{-1}$	[17]
6.	HPLC	UV, $\lambda = 240$ nm	0.01 $\mu\text{g mL}^{-1}$	0.1-100 $\mu\text{g mL}^{-1}$	[18]
7.	HPLC	HPLC-MS	1.0 $\text{ng mL}^{-1}$	0.001-10 $\mu\text{g mL}^{-1}$	[19]
8.	HPLC	HPLC-MS	0.007 $\mu\text{g mL}^{-1}$	0.01-20 $\mu\text{g mL}^{-1}$	[20]
9.	HPLC	Electrochemical	0.5 $\mu\text{g mL}^{-1}$	5-100 $\mu\text{g mL}^{-1}$ or 0.5-50 $\mu\text{g mL}^{-1}$	[21]
10.	HPLC	UV, $\lambda = 282$ nm	0.5 $\mu\text{g mL}^{-1}$	-	[22]
11.	HPLC	UV, $\lambda = 214$ nm	100 $\text{ng mL}^{-1}$	1-50 $\mu\text{g mL}^{-1}$	[23]
12.	HPLC	UV, $\lambda = 225$ nm	0.52 $\mu\text{g mL}^{-1}$	1-100 $\mu\text{g mL}^{-1}$	[24]
13.	HPLC	UV, $\lambda = 198$ nm	0.03 $\mu\text{g mL}^{-1}$	-	[25]
14.	HPLC	UV, $\lambda = 240$ nm	0.4 $\mu\text{g mL}^{-1}$	-	[26]
15.	HPLC	UV, $\lambda = 230$ nm	30.0 $\text{ng mL}^{-1}$	-	[27]
16.	HPLC	UV, $\lambda = 230$ nm	0.5 $\mu\text{g mL}^{-1}$	1-200 $\mu\text{g mL}^{-1}$	[28]
17.	HPLC	UV, $\lambda = 228$ nm	1.0 $\mu\text{g mL}^{-1}$	2-50 $\mu\text{g mL}^{-1}$	[29]
18.	HPLC	UV, $\lambda = 229$ nm	1.0 $\mu\text{g mL}^{-1}$	-	[30]
19.	HPLC	UV, $\lambda = 229$ nm	0.2 $\mu\text{g mL}^{-1}$	-	[31]
20.	HPLC	UV, $\lambda = 230$ nm	0.8 $\mu\text{g mL}^{-1}$	-	[32]
21.	HPLC	UV, $\lambda = 215$ nm	0.5 $\mu\text{g mL}^{-1}$	0.5-100 $\mu\text{g mL}^{-1}$	[33]

**Table 1**  
SPECTROPHOTOMETRIC AND HPLC  
ANALYTICAL METHODS FOR  
QUANTIFICATION OF VCM

(xGnP) and oxidized exfoliated graphite nanoplatelets (ox-xGnP) present high adsorption capacity for vancomycin, which can be applied in preconcentration steps, in clinical studies for monitoring of VCM level in biological fluids. Because of graphite nanoparticles aggregation and possible VCM dimerization, an ultrasonic treatments for good dispersion being necessary.

#### Analytical methods for the determination of VCM

Vancomycin hydrochloride is officially recognized in British Pharmacopeia (BP) [8] and United States Pharmacopeia (USP) [9]. Official methods used for VCM quantification, are usually based on microbiological methods, when the potency of an antibiotic is estimated by comparison of growth inhibition between sample with known concentrations of antibiotic and reference standard solutions [8].

A survey of literature revealed that few quantitative analytical spectrophotometric methods (UV-VIS) for VCM have been reported. Other methods include high performance liquid chromatography (HPLC), polarography [10], capillary electrophoresis (CE) [11], radioimmunoassay (RI) [12], fluorescence polarization immunoassay (FPI) [7, 13], and flow injection analysis (FIA) [14, 15]. Some of the analytical spectrophotometric and HPLC methods, described in the literature for vancomycin determination in pharmaceutical preparations and biological fluids, are presented below in table 1.

Spectrophotometric analytical methods are recommended for their low cost and simplicity. Due to molecular complexity of VCM, in literature there are described only few methods which use this technique. In many cases, it is necessary to heat the samples, this leading to VCM degradation, especially for low concentrations of antibiotic solutions. It is noticed that HPLC methods used for the determination of VCM, include UV detection in the

range of wavelength between 198 and 282 nm (table 1). For the analysis of pharmaceutical products, detection limits obtained by spectrophotometric methods are comparable with those obtained by HPLC methods.

Some methods need preliminary procedures for extraction and preconcentration of samples containing analytes in complex matrices, or to remove possible interferences. For some methods, serum and urine samples are analysed using a preparative chromatographic with an extraction column for VCM, followed by separation on reverse-phase chromatographic column and UV detection. Due to the pharmaceutical importance of VCM, its high toxicity level, and to avoid time consuming for preconcentrations, developing of more simple analytical methods becomes very important.

#### Experimental part

##### Equipment

-Spectra Suite UV-VIS spectrophotometer (Ocean Optics, USA) was used for recording all scan and absorbance measurements in 1cm quartz cells.

-Sensitive six digits analytical balance (Sartorius BL 210S, Germany).

-Portable pH-meter (Mettler Toledo, Switzerland).

-Ultrasonic bath Elma P-30H (Elma Schmidbauer GmbH, Germany).

-FTIR Spectrum GX (Perkin Elmer, Germany).

-Thermogravimetric Analyzer TGA /SDTA 851 (Mettler Toledo, Switzerland).

##### Reagents and solutions

All the chemicals were of analytical grade and all the aqueous solutions were prepared with distilled water. Vancomycin hydrochloride (active substance) in powder, of pharmaceutical grade was obtained from Sigma-Aldrich, Germany. Freshly prepared solutions were always used.

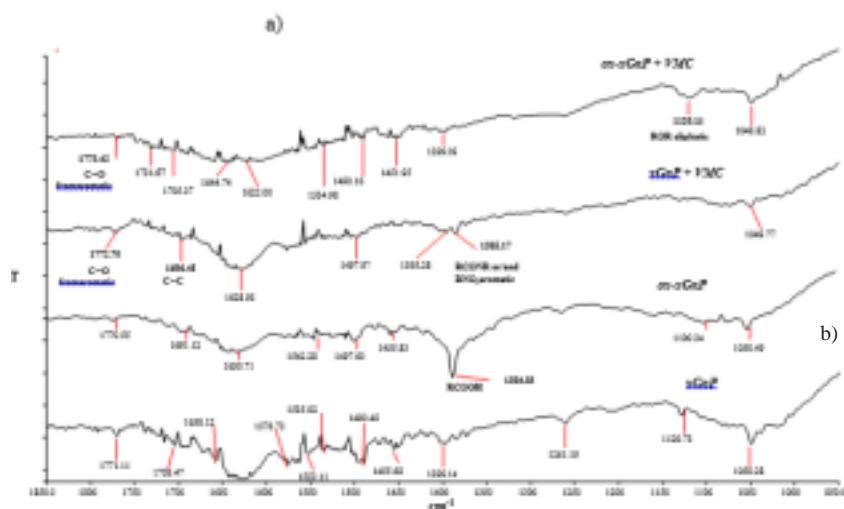
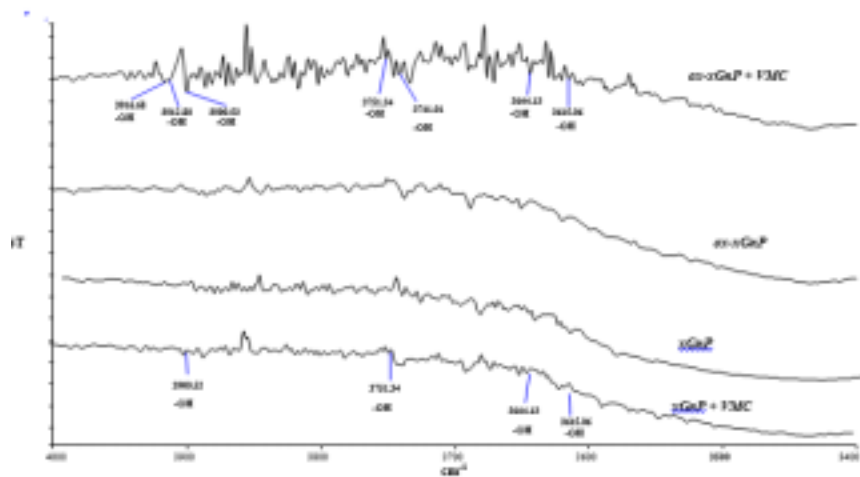


Fig. 2. Comparative FTIR spectra obtained for ox-xGnP, xGnP, xGnP + VCM and ox-xGnP + VCM in the spectral range: a) 4000 – 3400  $\text{cm}^{-1}$  and b) 1900 – 950  $\text{cm}^{-1}$

Methanol of spectrometric purity was obtained from Sigma-Aldrich, Germany. Commercially available exfoliated graphite nanoplatelets (xGnP), with diameters of 15 nm and medium length  $< 0.01\mu\text{m}$  were bought from XG Sciences, Inc. East Lansing, Michigan, MI 48823, USA. Pristine xGnP was functionalized by oxidation, in order to obtain oxidized exfoliated graphite nanoplatelets (ox-xGnP), according to Hummers' method [34].

#### Preparation of ox-xGnP + VCM and xGnP + VCM sample solutions

In order to achieve the proposed experiments, stock solutions of nanomaterial were prepared by dispersion of 0.25 mg xGnP / ox-xGnP in 25 mL methanol, followed by ultrasonic treatment at 25°C for 30 min. In each 10 mL volume marked quotted flasks it was transferred 1.0 mL stock solution of nanomaterial, and respectively 1.0, 1.5, 2.0, 2.5 and 3.0 mL standard solution of 100  $\text{mg mL}^{-1}$  VCM. The volume of each flask was completed to the mark with distilled water in order to obtain 10, 15, 20, 25 and 30  $\text{mg mL}^{-1}$  VCM. These solutions were transferred in 25 mL centrifuge tubes.

#### Preparation of (ox-xGnP + VCM) and (xGnP + VCM) complex

10 mg of xGnP / ox-xGnP were dispersed in 10 mL distilled water by sonication at 35 Hz frequency and 25°C. After one hour, 100  $\mu\text{g}$  VCM were added and ultrasound treatment was applied for others 2 h at 25°C, to complete the adsorption of the antibiotic on pristine or oxidized exfoliated graphite nanoplatelets. The impregnated material was separated by centrifugation at 4000 rpm, for 20 min at 4°C, and dried in a nitrogen atmosphere. The

obtained samples were used for characterization by specific techniques.

#### Spectrophotometric method of analysis

In this study a spectrophotometric method of analysis was developed, without derivatization and the adsorbances of supernatant obtained after centrifugation of the solutions were measured at 220 nm, in 1 cm quartz cuvette against a mixture of water: methanol (9:1) (v/v), as blank solution.

#### Adsorption procedure

Adsorption experiments of solutions prepared as described at section 2.3. In 25 mL centrifuge tubes, there were carried out for 3 h maximum contact time, using an ultrasonic bath (Elma P-30H Ultrasonic), at 37 Hz, with 30 min testing frequency. After centrifugation at 4000 rpm, for 20 min at 4°C, the pH of the solutions was checked out and the absorbance at 220 nm was measured. In order to determine minimum time requested for maximum adsorption and the influence of temperature, kinetics was studied at three different temperatures: 20, 25 and 30°C.

## Results and discussions

### Characterization of the nanomaterials (FTIR, TGA, SEM)

#### Fourier transformed infrared spectroscopy (FTIR)

FTIR spectra of simple or of impregnated nanomaterials were registered on FTIR Spectrum GX (Perkin Elmer), by transmission technique using KBr discs, in the range 4000 - 400  $\text{cm}^{-1}$ . There were observed spectral variations including broadening, shifting and reduction in relative intensities, these being considered as a confirmation of the complex formation. The comparative spectra, in two relevant ranges, are presented in figure 2.

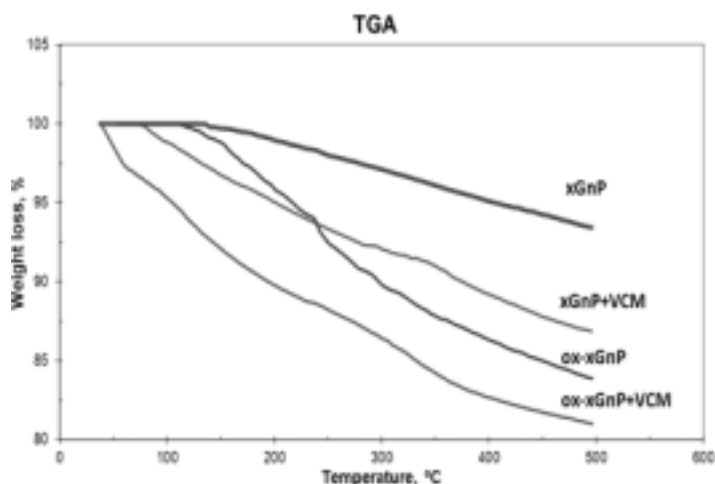


Fig. 3. Comparative thermograms for xGnP and xGnP + VCM, ox-xGnP and ox-xGnP + VCM

The absorption bands in between  $3916\text{ cm}^{-1}$  and  $3615\text{ cm}^{-1}$  can be attributed to hydroxyl groups  $-\text{OH}$  and/or  $-\text{NH}$  and proves the formation of hydrogen bonds between hydroxyl/ amino groups of VCM and the hydrophilic groups of the nanomaterial, especially for ox-xGnP. Adsorbed VCM modifies the spectra of the nanomaterials, bands at  $1885\text{ cm}^{-1}$ ,  $1867\text{ cm}^{-1}$ ,  $1772\text{ cm}^{-1}$ ,  $1696\text{ cm}^{-1}$  and at  $672\text{ cm}^{-1}$ , being specific for double bonds  $\text{C}=\text{C}$ , anhydrides, benzene rings overtones,  $\text{C}=\text{O}$  from aromatics, substitutes benzene rings and secondary amides. The intensity of the band at  $1384\text{ cm}^{-1}$  is characteristic for carboxylic groups  $\text{R}-\text{COOH}$  and/or aldehydic groups  $\text{R}-\text{CHO}$ , for oxidized nanoplatelets. These bands present low intensities for the complex of ox-xGnP + VCM, due to the chemical interactions. The vibration band observed at  $1119\text{ cm}^{-1}$  corresponds to  $\text{R}-\text{O}-\text{R}$  aliphatic ether.

It clearly appear vibration bands in the range  $4000 - 3400\text{ cm}^{-1}$  observed in figure 2a, with maximum peaks at  $3916\text{ cm}^{-1}$ ,  $3912\text{ cm}^{-1}$ ,  $3900\text{ cm}^{-1}$ ,  $3751\text{ cm}^{-1}$ ,  $3741\text{ cm}^{-1}$ ,  $3644\text{ cm}^{-1}$  and  $3615\text{ cm}^{-1}$ , for the complex (ox-xGnP + VCM), and at  $3900\text{ cm}^{-1}$ ,  $3751\text{ cm}^{-1}$ ,  $3644\text{ cm}^{-1}$  and  $3615\text{ cm}^{-1}$  for the complex (xGnP + VCM), respectively. These bands can be attributed to the existence of hydrogen bonds between hydroxyl groups  $-\text{OH}$  from VCM and hydrophilic groups of nanomaterial, especially for ox-xGnP. In addition, the peak at  $1772\text{ cm}^{-1}$ , observed in figure 2b, indicates the existence of  $\text{C}=\text{O}$  bond from the aromatic rings, that might be due to the  $\pi-\pi$  interactions of VCM with the graphene planes. Changes of intensities at  $1384\text{ cm}^{-1}$  are due to  $\text{R}-\text{CO}-\text{NR}$  amidic bond, proving the interaction between amino groups of VCM and  $\text{R}-\text{COOH}$  from functionalized graphene (ox-xGnP). The vibration band observed at  $1120\text{ cm}^{-1}$  corresponds to  $\text{R}-\text{O}-\text{R}$  aliphatic eter.

#### Thermogravimetric analysis (TGA)

The dynamic of weight loss tests were conducted in  $100\text{ }\mu\text{L}$   $\text{Al}_2\text{O}_3$  melting, under purge of  $\text{N}_2$ , on a sample with average weights of  $10\text{ mg}$  (ox-xGnP + VCM) / (xGnP + VCM) in a temperature range  $50 - 500^\circ\text{C}$ , with a scan rate

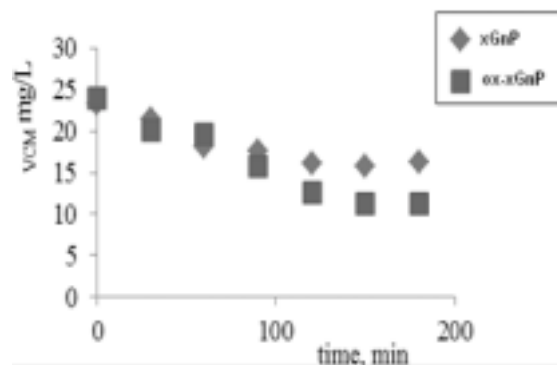


Fig. 4. Effect of the contact time on the adsorption of VCM on xGnP and ox-xGnP. Conditions:  $\text{pH}=7.0$ , temperature  $293\text{ K}$ , initial VCM concentration  $25\text{ mg L}^{-1}$ , amount of xGnP, or ox-xGnP  $0.01\text{ mg}$ , volume of solution  $10\text{ mL}$

of  $1^\circ\text{C}/\text{min}$ . The thermogravimetric experiments conducted on pristine and oxidized xGnP, before and after VCM adsorption, are presented in figure 3.

As expected, the thermal degradation of xGnP is a multistage process. Till  $110^\circ\text{C}$  ox-xGnP has a mass loss of  $0.2\%$ , due to the evaporation of adsorbed water. In the same temperature range, the mass loss of the complex (ox-xGnP+VCM) is  $5.3\%$ , and can be attributed to VCM adsorption. From  $110$  to  $500^\circ\text{C}$  it was registered a mass difference of  $9.6\%$ , due to the decarboxylation of the carboxylic groups present at the xGnP edges. The residue obtained at  $500^\circ\text{C}$  was calculated to be  $86.8\%$  for the sample with VCM and  $80.9\%$  for ox-xGnP, respectively and can be attributed to the elimination of hydroxyl groups. The comparative thermogravimetric diagrams from figure 3 show that the mass percentage of (xGnP + VCM) is  $3.7\%$  higher comparing to xGnP. The residues obtained at  $500^\circ\text{C}$  calculated for a sample with VCM were  $86.8$  and  $93.3\%$  xGnP, respectively. The mass losses can be explained based on the thermal oxidation of the remaining disordered carbon. The residue in percentage represents the difference between  $100$  and total sample mass loss.

#### Sorption studies

The samples solutions with five different concentrations of VCM, prepared according to the procedure described at section 2.3. (Preparation of (ox-xGnP + VCM) and xGnP + VCM) sample solutions), were tested. The effect of contact time, temperature, adsorption kinetics and thermodynamics were investigated for understanding the mechanism of adsorption.

The effect of the contact time on the adsorption of VCM on xGnP and ox-xGnP was studied and it is presented in figure 4.

It can be observed that the adsorption capacity of both xGnP and ox-xGnP increased in the first two hours and then decreases not very fast. Based on these experiments, a contact time of two hours was selected for the adsorption equilibrium in further adsorption studies. To investigate the

Kinetic Models	Functional Form
Lagergren model	$\frac{dq}{dt} = k(q_e - q_t)$ (1)
Kavitha and Namasiyayam model	$q = k_1 t^{1/2} + C$ (2)
Pseudo-second order model	$\frac{dq}{dt} = k(q_e - q_t)^2$ (3)
Variables in the kinetics equations: $q_e$ - amount of solute adsorbed at equilibrium, (mg/g) ; $q_t$ - amount of solute adsorbed at any given time "t", (mg/g) ; C - concentration of sorbate in the solution at any given time "t"	

Table 2  
THE EQUATIONS OF  
SEVERAL KINETIC MODELS

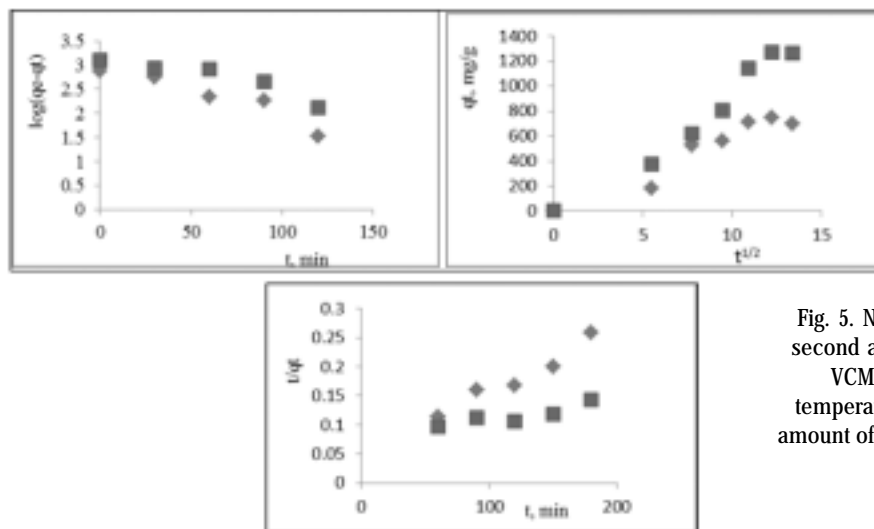


Fig. 5. Non-linear kinetic models: pseudo-first, pseudo-second and intra-particle diffusion for the adsorption of VCM on xGnP and ox-xGnP. Conditions: pH=7.0, temperature 293 K, initial VCM concentration 25 mg L<sup>-1</sup>, amount of xGnP or ox-xGnP 0.01 mg, volume of solution 10 mL

Kinetic model	qe, mg/g		k		R <sup>2</sup>	
	xGnP	ox-xGnP	xGnP	ox-xGnP	xGnP	ox-xGnP
Pseudo-first order	26.68	44.03	0.0056	0.0056	0.925	0.964
Pseudo-second order	76.92	35.71			0.896	0.967
Intra-particle diffusion	57.78	120	58.07	130.5	0.965	0.999

**Table 3**  
KINETIC PARAMETERS FOR THE ADSORPTION OF VCM ON xGnP AND ox-xGnP FOR A VCM CONCENTRATION OF 20 mg L<sup>-1</sup>

adsorption mechanism, three kinetic models (pseudo-first order, pseudo-second order and intra-particle diffusion) were applied.

The kinetic parameters and correlation coefficients for VCM removal by xGnP and ox-xGnP are summarised in table 3. The correlation coefficient R<sup>2</sup> present the best value for the pseudo-second-order model. All the other results indicate that pseudo-second-order kinetic model fit the adsorption of VCM on both xGnP and ox-xGnP.

The adsorption isotherm models indicate the possible interactions between adsorbent and adsorbate at the equilibrium of the adsorption process. From linearized adsorption isotherms, Langmuir 1, Langmuir 2 and Freundlich it can be observed that the adsorption capacity of xGnP and ox-xGnP increased by increasing the equilibrium concentration of VCM, probably because the increase of VCM concentration improves the diffusion of VCM molecules onto xGnP sheets.

The Langmuir model assumes that the adsorption is based on monolayer coverage and no interaction between adsorbed species. From equation (5) of the model, the Langmuir constant K<sub>L</sub>, which is related to the affinity of the binding sites and the maximum adsorption q<sub>m</sub>, which represents the maximum adsorption capacity of the adsorbent can be calculated. The Freundlich model is an empirical model based on multilayer adsorption on heterogeneous surfaces. From equation (4) of the model, the Freundlich constants can be calculated. K<sub>F</sub> represents the adsorption capacity and n represents the adsorption strength. The magnitude of n quantifies the adsorption process and the heterogeneity of the surface. If n is bigger

than 1, a favourable adsorption process takes place, proving a good adsorption capacity.

The relative parameters calculated from Langmuir and Freundlich models are listed in table 5. It can be observed that the Langmuir model fitted better on the adsorption data in comparison with Freundlich one, proving that VCM adsorption on xGnP and ox-xGnP is a monolayer one, probably due also to the dimensions of the VCM molecule, which influence q<sub>m</sub> value of both xGnP and ox-xGnP, of 1000 mg/g independent of the oxygen containing groups, but dependent on the same surface area of the carbon-based nanostructures.

The effect of the temperature was studied in the range 293-303K, at three temperatures. The following experimental conditions were used: pH = 7.0, amount of xGnP, or ox-xGnP = 0.01 mg, volume of solution = 10 mL, initial concentration of VCM = 25 mg L<sup>-1</sup>. It was observed that the adsorption capacity of VCM onto xGnP and ox-xGnP decreased by increasing temperature, suggesting an exothermic process. This may be due to a tendency for the VCM molecules to migrate from the solid adsorbent in solution with an increase of the solution temperature.

Thermodynamic considerations are necessary to characterize the process. The standard Gibbs free energy change ΔG<sup>0</sup> is an important criterion of the spontaneity of the chemical reaction. Reactions occur spontaneously at a given temperature, if ΔG<sup>0</sup> presents negative values, its values being calculated based on the equation:

$$\Delta G^0 = -RT \ln K_a \quad (6)$$

where:

**Table 4**  
THE EQUATIONS OF FREUNDLICH AND LANGMUIR ISOTHERMS. WHERE: C<sub>e</sub> - EQUILIBRIUM CONCENTRATION; C<sub>s</sub> - ADSORBATE SOLUBILITY AT A GIVEN TEMPERATURE; E<sub>0</sub> - SOLID CHARACTERISTIC ENERGY TOWARDS A REFERENCE COMPOUND; q<sub>e</sub> - ADSORBED AMOUNT; q<sub>max</sub> - SATURATED MONOLAYER SORPTION CAPACITY; K<sub>F</sub> - FREUNDLICH CONSTANT, mg/g; 1/n - FREUNDLICH CONSTANT INDICATING ADSORPTION INTENSITY; K<sub>L</sub> - LANGMUIR CONSTANT, L/mg

Isotherm	Functional form
Freundlich	$q_e = K_F C_e^{1/n}$ (4)
Langmuir	$q_e = q_{max} \frac{K_L C_e}{1 + K_L C_e}$ (5)

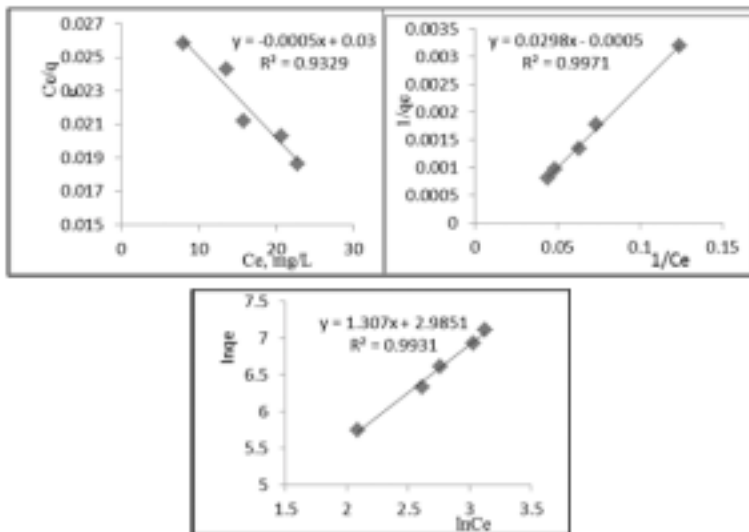


Fig. 6. Adsorption isotherms Langmuir 1, Langmuir 2 and Freundlich of VCM onto xGnP at different initial VCM concentrations. Conditions: pH=7.0, temperature 293 K, amount of xGnP or ox-xGnP 0.01 mg, volume of solution 10 mL.

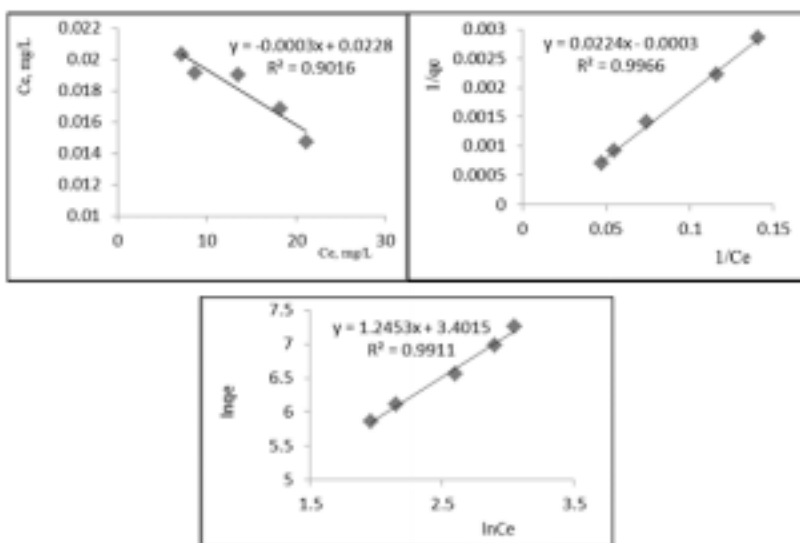


Fig. 7. Adsorption isotherms Langmuir 1, Langmuir 2 and Freundlich of VCM onto ox-xGnP at different initial VCM concentrations. Conditions: pH=7.0, temperature 293 K, amount of xGnP or ox-xGnP 0.01 mg, volume of solution 10 mL.

Adsorption isotherm model	Isotherm parameters					
	$K_L(L/g)$		$q_m(mg/g)$		$R^2$	
Langmuir 1	xGnP	ox-xGnP	xGnP	ox-xGnP	xGnP	ox-xGnP
	0.033	0.045	1000	1000	0.932	0.901
Langmuir 2	xGnP	ox-xGnP	xGnP	ox-xGnP	xGnP	ox-xGnP
	0.034	0.045	1000	1000	0.997	0.996
Freundlich	$K_F(mg/g)$		$n$		$R^2$	
	xGnP	ox-xGnP	xGnP	ox-xGnP	xGnP	ox-xGnP
	19.60	20.90	1.315	1.245	0.993	0.991

Table 5  
ISOTHERM PARAMETERS  
FOR THE ADSORPTION OF  
VCM ON xGnP AND  
ox-xGnP AT 20 °C

$K_a$  is the sorption equilibrium constant;  
 $\Delta G^0$  is the standard free energy change, J/mol;  
 $R$  is the universal gas constant 8314 J/mol K;  
 $T$  is the absolute temperature, K.  
 The free Gibbs energy  $\Delta G^0$  can be also represented as:

$$\Delta G^0 = \Delta H^0 - T\Delta S^0 \quad (7)$$

where adsorption enthalpy  $\Delta H^0$  and adsorption entropy  $\Delta S^0$  at different temperatures, are calculated based on the equations:

$$K_L = q_e/C_e \quad (8)$$

$$\ln K_L = \Delta S^0/R - \Delta H^0/RT \quad (9)$$

where:

$q_e$  is the amount of adsorbed VCM;  
 $C_e$  is the equilibrium concentration;  
 $R$  is the universal gas constant 8314 J/mol K;  
 $T$  is the absolute temperature, K.  $\Delta H^0$  and  $\Delta S^0$  are calculated from the intercept and the slope of Van't Hoff linear plot  $\ln K_L$  vs.  $1/T$ .

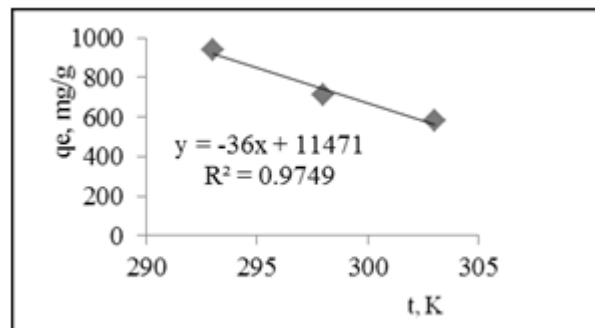


Fig. 8. Effect of the temperature on the VCM sorption on ox-xGnP

The correlation of the experimental data conducted to assess the best isotherm equation, which describes the VCM sorption on xGnP / ox-xGnP. Based on these results and taking into account the complicated structure of VCM, the adsorption mechanism was explained based on  $\pi$ - $\pi$ . VCM contains  $\pi$  electrons which interact with the  $\pi$  electrons from xGnP, the influence of oxygen containing

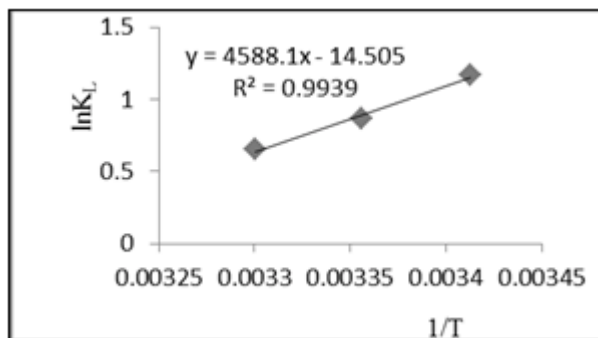


Fig. 9. Thermodynamic parameters of the adsorption of VCM on ox-xGnP in the following conditions:  $pH=7.0$ , temperatures 293 – 303 K, amount of xGnP or ox-xGnP 0.01 mg, volume of solution 10 mL, initial concentration of VCM 25 mg L<sup>-1</sup>.

groups being less important in this case. There can be sorbent-sorbate interactions of  $\pi - \pi$  type between the xGnP pristine and oxidized planes and the benzene rings from VCM molecule and there can appear in ox-xGnP hydrogen bonds between VCM and the oxygen containing groups at the edges of xGnP. These last bonds can be hindered by the big dimensions of the VCM molecule.

### Conclusions

Experimental data obtained showed that exfoliated graphite nanoplatelets (xGnP) interact very well with vancomycin molecules. It was noticed that ox-xGnP retain better VCM comparing to xGnP, with the same adsorption rate. Functionalizations by oxidation, ox-xGnP nanosheets have a higher adsorbance capacity of VCM, due to the active groups on the surface area. The required contact time to reach the adsorption equilibrium was about 120 min in both cases. The study in aqueous solutions was completed in different experimental conditions to demonstrate the adsorption properties of nanomaterials and the affinity of VCM for this type of surface area. The results showed that process conditions at  $pH$  near 7.00 (like physiological  $pH$ ), and low temperature (20-25°C) are most favourable.

The interactions between VCM and xGnP/ox-xGnP, were investigated using FTIR and thermogravimetry of binary system (xGnP + VCM) and (ox-xGnP + VCM) after adsorption.

The experimental results prove the fact that xGnP and ox-xGnP are compatible with VCM, and could be a very promising alternative for extraction and concentration of this drug from biological samples, before quantitative analysis.

### References

- SWEETMAN, S. C.; "Martindale, the Complete Drug Reference", 36th Ed, 2009.
- BAUER, L. A.; "Applied Clinical Pharmacokinetics", 2nd Ed, McGraw-Hill Companies, USA, 2008.
- GIGUERE, S.; PRESCOTT, J. F.; BAGGOT, J. D.; WALKER, R. D.; DOWLING, P. M.; "Antimicrobial Therapy in Veterinary Medicine", 4th Ed, Blackwell Publishing, USA, 2006.
- REYNOLDS, J.E.F.; "Martindale the Extra Pharmacopoeia", The Pharmaceutical Press, London, 1996, p. 295.
- HAMMETT-STABLER, C. A.; JOHNS, T.; Clin. Chem. no. 44, 1998, p. 1129.

- DAVANI, S.; MURET, P.; ROYER, B.; HOEN, B.; KANTELI, J. P.; Ann. Biol. Clin. no. 60, 2002, p. 655.
- TOBIN, C. M.; DARVILLE, J. M.; THOMSON, A. H.; SWEENEY, G.; WILSON, J. F.; MACGOWAN, A. P.; WHITE, L.O.; J. Antimicrob. Chemother. no. 50, 2002, p. 713.
- \*\*\* The Stationary Office on behalf of the Medicines and Healthcare Products Regulatory Agency (MHRA), "British Pharmacopoeia", Version 17, 7th Ed, London, 2013.
- \*\*\* U. S. Pharmacopoeial Convention, "United States Pharmacopoeia 30, NF 25", Rockville, USA, 2007.
- BELAL, F.; EL-ASHRY, S. M.; EL-KERDAWY, M. M.; EL-WASSEEF, D. E.; Arzneim. Forsch no. 51, 2001, p. 763.
- KITAHASHI, T.; FURUTA, I.; Clin. Chim. Acta no. 312, 2001, p.221.
- ACKERMAN, B. H.; BERG, H. G.; STRATE, R. G.; ROSTSCHAFER, J. C.; J. Clin. Microbiol. no. 18, 1983, p. 994.
- HERMIDA, J.; ZAERA, S.; TUTOR, J. C.; Ther. Drug Monit. no. 23, 2001, p. 725.
- CHABENAT, C.; ANDRE, D.; BOUCLY, P.; Talanta no. 30, 1983, p. 963.
- VILA, M. M. D.; SALOMÃO, A. A.; TUBINO, M.; Ecl. Quím, São Paulo no. 33, 2008, p. 67.
- EL-ASHRY, S. M.; BELAL, F.; EL-KERDAWY, M. M.; ELWASSEEF, D. R.; Mikrochim. Acta no. 135, 2000, p. 191.
- SASTRY, C. S. P.; RAO, T. S.; RAO, P. S. N. H. ; PRASSA, U. V.; Mikrochim. Acta no. 140, 2002, p. 109.
- HOSOTSUBO, H. ; J. Chromatogr., B: Anal. Technol. Biomed. Life Sci. no.487, 1989, p.421.
- CASS, T. R.; VILLA, J. S.; KARR, D.E.; SCHMIDT Jr, D. E.; Rapid Commun.MassSpectrom. no. 15, 2001, p. 406.
- SHIBATA, N.; ISHIDA, M.; PRASAD, Y. V. R.; GAO, W.; YOSHIKAWA, Y.; TAKADA, K.; J. Chromatogr., B: Anal. Technol. Biomed. Life Sci. no. 789, 2003, p. 211.
- FAVETTA, P.; GUITON, J.; BLEYZAC, N.; DUFRESNE, C.; BUREAU, J.; J. Chromatogr., B: Anal. Technol. Biomed. Life Sci. no. 751, 2001, p. 377.
- FARIN, D.; PIVA, G. A.; GOZLAN, I.; KITZES-COHEN, R.; J. Pharm. Biomed. Anal. no. 18, 1990, p. 367.
- JEHL, F.; GALLION, C.; THIERRY, R. C.; MONTEIL, H.; Antimicrob. Agents Chemother. no. 27, 1985, p. 503.
- LI, L.; MILES, M. V.; HALL, W.; CARSON, S.; Ther. Drug Monit. no. 17, 1995, p. 366.
- DEL NOZAL, M. J.; BERNAL, J. L.; PAMPLIEGA, A.; MARINERO, P.; LÓPEZ, M. I.; COCO, R.; J. Chromatogr. A no. 727, 1996, p. 231.
- PLOCK, N.; BUERGER, C.; KLOFT, C.; Biomed. Chromatogr. no. 19, 2005, p. 237.
- FORLAY-FRICK, P.; NAGY, Z. B.; FEKETE, J.; KETTRUP, A.; GEBEFUGI, I.; J. Liq. Chromatogr. Relat. Technol. no. 24, 2001, p. 497.
- SANTOS, C. R.; FEFERBAUM, R.; PAULA, M. L. S. A.; BERTOLINE, M. A.; OMOSAKO, C. E. K.; SANTOS, S. R. C. J.; Rev. Bras. Ciências Farmac. no. 37, 2001, p. 87.
- DEMOTES-MAINARD, F.; LABAT, L.; VINCON, G.; BAINNWARTH, B.; Ther. Drug Monit. no. 16, 1994, p. 293.
- BAUCHET, J.; PUSSARD, E.; GARAUD, J. J.; J. Chromatogr. no. 414, 1987, p. 472.
- LUKSA, J.; MARUSIC, A.; J. Chromatogr. B: Anal. Technol. Biomed. Life Sci. no. 667, 1995, p. 227.
- BELLI, C. V.; Dissertação de Mestrado, Universidade de São Paulo, Brasil, 2000.
- SAITO, M.; SANTA, T.; TSUNODA, M.; HAMAMOTO, H.; USUI, N.; Biomed. Chromatogr. no. 18, 2004, p. 735.
- HUMMERS, W. S.; OFFEMAN, R. E.; J. Am. Chem. Soc. no. 80, 6, 1958, p. 1339

Manuscript received: 5.10.2015